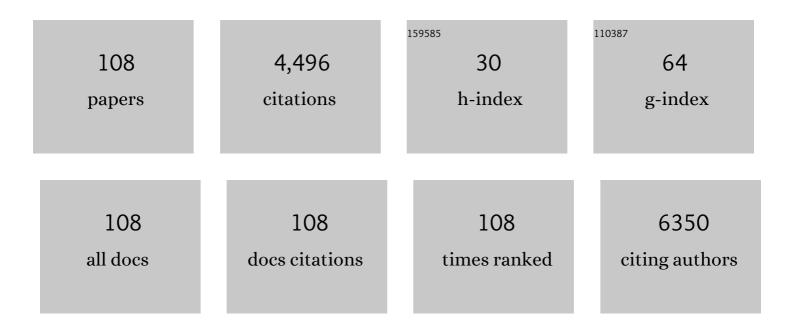


List of Publications by Year in descending order

Source: https://exaly.com/author-pdf/6675718/publications.pdf Version: 2024-02-01



YONG NI

#	Article	IF	CITATIONS
1	Tunable spatially dependent wrinkling morphologies on pre-curved surfaces. Extreme Mechanics Letters, 2022, 50, 101551.	4.1	6
2	A Prestressing Strategy Enabled Synergistic Energyâ€Đissipation in Impactâ€Resistant Nacre‣ike Structures. Advanced Science, 2022, 9, e2104867.	11.2	16
3	Biomimetic discontinuous Bouligand structural design enables high-performance nanocomposites. Matter, 2022, 5, 1563-1577.	10.0	27
4	Extremely fast-charging lithium ion battery enabled by dual-gradient structure design. Science Advances, 2022, 8, eabm6624.	10.3	50
5	High-Performance Liquid Metal/Polyborosiloxane Elastomer toward Thermally Conductive Applications. ACS Applied Materials & amp; Interfaces, 2022, 14, 21564-21576.	8.0	23
6	Effect of plasticity on voltage decay studied by a stress coupled phase field reaction model. Extreme Mechanics Letters, 2021, 42, 101152.	4.1	7
7	Nacreous aramid-mica bulk materials with excellent mechanical properties and environmental stability. IScience, 2021, 24, 101971.	4.1	15
8	High rate capability composite particles with root-inspired hierarchical channel structure. Journal of Power Sources, 2021, 494, 229777.	7.8	1
9	Ordered ring-shaped cracks induced by indentation in metal films on soft elastic substrates. Physical Review E, 2020, 102, 022801.	2.1	2
10	Impact of ridge cracking on the morphology of buckle-delamination. International Journal of Non-Linear Mechanics, 2020, 126, 103561.	2.6	2
11	Elastic interaction between inclusions and tunable periodicity of superlattice structure in nanowires. Applied Mathematics and Mechanics (English Edition), 2020, 41, 1461-1478.	3.6	1
12	Discontinuous fibrous Bouligand architecture enabling formidable fracture resistance with crack orientation insensitivity. Proceedings of the National Academy of Sciences of the United States of America, 2020, 117, 15465-15472.	7.1	96
13	Tunable hierarchical wrinkling: From models to applications. Journal of Applied Physics, 2020, 127, .	2.5	46
14	An analytical study on the morphology of buckle-delamination under large compression and boundary undulation. International Journal of Solids and Structures, 2020, 193-194, 557-567.	2.7	6
15	Real-Time Visualization of Solid-Phase Ion Migration Kinetics on Nanowire Monolayer. Journal of the American Chemical Society, 2020, 142, 7968-7975.	13.7	10
16	Growth modes of quasicrystals involving intermediate phases and a multistep behavior studied by phase field crystal model. Physical Review Materials, 2020, 4, .	2.4	4
17	A Nacreâ€Inspired Separator Coating for Impactâ€Tolerant Lithium Batteries. Advanced Materials, 2019, 31, e1905711.	21.0	71
18	Localization of wrinkle patterns by crack-tip induced plasticity: Experiments and simulations. International Journal of Solids and Structures, 2019, 178-179, 108-119.	2.7	4

#	Article	IF	CITATIONS
19	Hierarchical wrinkles and oscillatory cracks in metal films deposited on liquid stripes. Physical Review E, 2019, 99, 062802.	2.1	11
20	Diatomite derived hierarchical hybrid anode for high performance all-solid-state lithium metal batteries. Nature Communications, 2019, 10, 2482.	12.8	96
21	Biomimetic Carbon Tube Aerogel Enables Super-Elasticity and Thermal Insulation. CheM, 2019, 5, 1871-1882.	11.7	136
22	Controlled Wrinkling Patterns in Periodic Thickness-Gradient Films on Polydimethylsiloxane Substrates. Langmuir, 2019, 35, 7146-7154.	3.5	18
23	Growth of curved crystals: competition between topological defect nucleation and boundary branching. Soft Matter, 2019, 15, 4391-4400.	2.7	5
24	Fracture modes and hybrid toughening mechanisms in oscillated/twisted plywood structure. Acta Biomaterialia, 2019, 91, 284-293.	8.3	40
25	Interaction between capped tetrahedral gold nanocrystals: dependence on effective softness. Soft Matter, 2019, 15, 8392-8401.	2.7	4
26	Hierarchical crack patterns of metal films sputter deposited on soft elastic substrates. Physical Review E, 2019, 100, 052804.	2.1	8
27	Interfacial strength-controlled energy dissipation mechanism and optimization in impact-resistant nacreous structure. Materials and Design, 2019, 163, 107532.	7.0	43
28	Understanding size-dependent migration of a two-phase lithiation front coupled to stress. Acta Mechanica, 2019, 230, 303-317.	2.1	9
29	Rapid Programmable Nanodroplet Motion on a Strain-Gradient Surface. Langmuir, 2019, 35, 2865-2870.	3.5	19
30	Ring-shaped buckles in metal films induced by evaporation of micro-scaled silicone oil droplets. Thin Solid Films, 2018, 651, 131-137.	1.8	4
31	Phase field model for two-phase lithiation in an arbitrarily shaped elastoplastic electrode particle under galvanostatic and potentiostatic operations. International Journal of Solids and Structures, 2018, 143, 73-83.	2.7	25
32	Improved phase field model of dislocation intersections. Npj Computational Materials, 2018, 4, .	8.7	16
33	Woodâ€Inspired Highâ€Performance Ultrathick Bulk Battery Electrodes. Advanced Materials, 2018, 30, e1706745.	21.0	205
34	Moisture-triggered actuator and detector with high-performance: interface engineering of graphene oxide/ethyl cellulose. Science China Materials, 2018, 61, 1291-1296.	6.3	14
35	Effects of ridge cracking and interface sliding on morphological symmetry breaking in straight-sided blisters. Journal of the Mechanics and Physics of Solids, 2018, 112, 637-649.	4.8	7
36	Analysis of optimal crosslink density and platelet size insensitivity in graphene-based artificial nacres. Nanoscale, 2018, 10, 556-565.	5.6	13

#	Article	IF	CITATIONS
37	Phase-field simulation of the coupled evolutions of grain and twin boundaries in nanotwinned polycrystals. Applied Mathematics and Mechanics (English Edition), 2018, 39, 1789-1804.	3.6	4
38	Tunable mosaic structures in van der Waals layered materials. Physical Chemistry Chemical Physics, 2018, 20, 25428-25436.	2.8	3
39	Harnessing fold-to-wrinkle transition and hierarchical wrinkling on soft material surfaces by regulating substrate stiffness and sputtering flux. Soft Matter, 2018, 14, 6745-6755.	2.7	24
40	Geometrical distortion leads to Griffith strength reduction in graphene membranes. Extreme Mechanics Letters, 2017, 14, 31-37.	4.1	22
41	Size dependent morphologies of brittle silicon nitride thin films with combined buckling and cracking. Acta Materialia, 2017, 127, 220-229.	7.9	20
42	The shape of telephone cord blisters. Nature Communications, 2017, 8, 14138.	12.8	37
43	Self-Assembly of Islands on Spherical Substrates by Surface Instability. ACS Nano, 2017, 11, 2611-2617.	14.6	14
44	Sphere-To-Tube Transition toward Nanotube Formation: A Universal Route by Inverse Plateau–Rayleigh Instability. ACS Nano, 2017, 11, 2928-2933.	14.6	11
45	Stress-mediated lithiation in nanoscale phase transformation electrodes. Acta Mechanica Solida Sinica, 2017, 30, 248-253.	1.9	8
46	Passengers' behavioral intentions towards congestion: Observational study of the entry restrictions at traffic bottleneck. KSCE Journal of Civil Engineering, 2017, 21, 2393-2402.	1.9	10
47	Modeling progressive interfacial debonding of a mud-crack film on elastic substrates. Engineering Fracture Mechanics, 2017, 177, 123-132.	4.3	13
48	Tuning interfacial patterns of molecular bonds via surface morphology. Soft Matter, 2017, 13, 5970-5976.	2.7	10
49	Mass production of bulk artificial nacre with excellent mechanical properties. Nature Communications, 2017, 8, 287.	12.8	293
50	Transition from Deceleration to Acceleration of Lithiation Front Movement in Hollow Phase Transformation Electrodes. Journal of the Electrochemical Society, 2017, 164, A3371-A3379.	2.9	4
51	Investigation on the dependence of flash point of diesel on the reduced pressure at high altitudes. Fuel, 2016, 181, 836-842.	6.4	11
52	Interface failure modes explain non-monotonic size-dependent mechanical properties in bioinspired nanolaminates. Scientific Reports, 2016, 6, 23724.	3.3	29
53	Morphomechanics of bacterial biofilms undergoing anisotropic differential growth. Applied Physics Letters, 2016, 109, .	3.3	31
54	Elastic properties of gold supracrystals: Effects of nanocrystal size, ligand length, and nanocrystallinity. Journal of Chemical Physics, 2016, 144, 144507.	3.0	16

#	Article	IF	CITATIONS
55	Size-dependent assembly of ligated gold nanocrystals in two dimensions. Journal of Physics Condensed Matter, 2016, 28, 445201.	1.8	1
56	Molecular dynamics simulation of interparticle spacing and many-body effect in gold supracrystals. Nanotechnology, 2016, 27, 135707.	2.6	15
57	Stress anisotropy controlled morphological evolution in core–shell nanowires. Extreme Mechanics Letters, 2016, 8, 160-166.	4.1	4
58	Controlled Formation of Surface Patterns in Metal Films Deposited on Elasticity-Gradient PDMS Substrates. ACS Applied Materials & Interfaces, 2016, 8, 5706-5714.	8.0	72
59	Alternative transmission mode and long stacking fault formation during a dissociated screw dislocation across a coherent sliding interface. Journal Physics D: Applied Physics, 2015, 48, 395301.	2.8	1
60	Phase field modeling of a glide dislocation transmission across a coherent sliding interface. Modelling and Simulation in Materials Science and Engineering, 2015, 23, 035002.	2.0	10
61	Effects of particle shape and concurrent plasticity on stress generation during lithiation in particulate Li-ion battery electrodes. Mechanics of Materials, 2015, 91, 372-381.	3.2	28
62	Strong Crack Blunting by Hierarchical Nanotwins in Ultrafine/Nano-grained Metals. Materials Research Letters, 2015, 3, 190-196.	8.7	11
63	Optimization design of strong and tough nacreous nanocomposites through tuning characteristic lengths. Journal of the Mechanics and Physics of Solids, 2015, 81, 41-57.	4.8	54
64	Tunable Formation of Ordered Wrinkles in Metal Films with Controlled Thickness Gradients Deposited on Soft Elastic Substrates. ACS Applied Materials & Interfaces, 2015, 7, 5160-5167.	8.0	69
65	Aggregation dynamics of molecular bonds between compliant materials. Soft Matter, 2015, 11, 2812-2820.	2.7	22
66	Variations of boundary reaction rate and particle size on the diffusion-induced stress in a phase separating electrode. Journal of Applied Physics, 2014, 116, 143506.	2.5	11
67	A coarse-grained simulation for tensile behavior of 2D Au nanocrystal superlattices. Nanotechnology, 2014, 25, 475704.	2.6	7
68	On the growth of buckle-delamination pattern in compressed anisotropic thin films. Acta Materialia, 2014, 69, 37-46.	7.9	31
69	Pumping through Porous Hydrophobic/Oleophilic Materials: An Alternative Technology for Oil Spill Remediation. Angewandte Chemie - International Edition, 2014, 53, 3612-3616.	13.8	253
70	Phase field modeling of flexoelectric effects in ferroelectric epitaxial thin films. Acta Mechanica, 2014, 225, 1323-1333.	2.1	38
71	Nonlinear analysis of compressed elastic thin films on elastic substrates: From wrinkling to buckle-delamination. International Journal of Solids and Structures, 2014, 51, 3715-3726.	2.7	64
72	Local-buckling-induced elastic interaction between inclusions in a free-standing film. International Journal of Solids and Structures, 2013, 50, 3742-3747.	2.7	7

#	Article	IF	CITATIONS
73	A Flexible and Highly Pressureâ€6ensitive Graphene–Polyurethane Sponge Based on Fractured Microstructure Design. Advanced Materials, 2013, 25, 6692-6698.	21.0	985
74	Phase field model of polarization evolution in a finite ferroelectric body with free surfaces. Acta Mechanica, 2013, 224, 1309-1313.	2.1	7
75	Modeling of ferroelectric control of magnetic domain pattern and domain wall properties. Journal of Applied Physics, 2013, 113, 134102.	2.5	7
76	Modeling of polar nanoregions dynamics on the dielectric response of relaxors. Journal of Applied Physics, 2013, 113, .	2.5	12
77	Effects of interface sliding on the formation of telephone cord buckles. Physical Review E, 2013, 88, 062405.	2.1	17
78	Role of modulus mismatch in vertically aligned nanocomposite formation during spinodal decomposition in constrained films. Applied Physics Letters, 2013, 103, 141903.	3.3	7
79	Thermodynamics and Kinetics of the Nanocheckerboard Formation. , 2013, , 193-202.		0
80	Spontaneous wrinkle branching by gradient stiffness. Physical Review E, 2012, 86, 031604.	2.1	31
81	A Family of Carbon-Based Nanocomposite Tubular Structures Created by <i>in Situ</i> Electron Beam Irradiation. ACS Nano, 2012, 6, 4500-4507.	14.6	34
82	Giant anhysteretic response of ferroelectric solid solutions with morphotropic boundaries: the role of polar anisotropy. Acta Mechanica Solida Sinica, 2012, 25, 429-440.	1.9	3
83	Large-area graphene realizing ultrasensitive photothermal actuator with high transparency: new prototype robotic motions under infrared-light stimuli. Journal of Materials Chemistry, 2011, 21, 18584.	6.7	111
84	Modeling kinetics of diffusion-controlled surface wrinkles. Physical Review E, 2011, 84, 051604.	2.1	29
85	Controllable buckling of an elastic disc with actuation strain. Europhysics Letters, 2010, 92, 16003.	2.0	4
86	Equivalency principle for magnetoelectroelastic multiferroics with arbitrary microstructure: The phase field approach. Journal of Applied Physics, 2010, 108, .	2.5	23
87	Spontaneous formation of vertically anticorrelated epitaxial islands on ultrathin substrates. Applied Physics Letters, 2010, 97, 261911.	3.3	14
88	Shape-dependent composition profile in epitaxial alloy quantum dots: A phase-field simulation. Computational Materials Science, 2010, 48, 871-874.	3.0	14
89	Modeling of magnetoelectric effect in polycrystalline multiferroic laminates influenced by the orientations of applied electric/magnetic fields. Journal of Applied Physics, 2009, 105, .	2.5	31
90	From chessboard tweed to chessboard nanowire structure during pseudospinodal decomposition. Nature Materials, 2009, 8, 410-414.	27.5	113

#	Article	IF	CITATIONS
91	Pseudospinodal Mode of Decomposition in Films and Formation of Chessboard-Like Nanostructure. Nano Letters, 2009, 9, 3275-3281.	9.1	49
92	Mechanism and conditions of the chessboard structure formation. Acta Materialia, 2008, 56, 4498-4509.	7.9	20
93	Giant magnetoelectric effect in sintered multilayered composite structures. Journal of Applied Physics, 2008, 104, .	2.5	68
94	Ferroelectric solid solutions with morphotropic boundaries: Vanishing polarization anisotropy, adaptive, polar glass, and two-phase states. Journal of Applied Physics, 2008, 103, .	2.5	218
95	Phase field simulation of crack tip domain switching in ferroelectrics. Journal Physics D: Applied Physics, 2007, 40, 1175-1182.	2.8	50
96	Phase field approach for strain-induced magnetoelectric effect in multiferroic composites. Journal of Applied Physics, 2007, 102, .	2.5	18
97	Cell morphology and migration linked to substrate rigidity. Soft Matter, 2007, 3, 1285.	2.7	58
98	The transformation sequences in the cubic→tetragonal decomposition. Acta Materialia, 2007, 55, 4903-4914.	7.9	51
99	Prediction of elastic properties of heterogeneous materials with complex microstructures. Journal of the Mechanics and Physics of Solids, 2007, 55, 517-532.	4.8	37
100	Phase Field Simulations of Hysteresis and Butterfly Loops in Ferroelectrics Subjected to Electro-Mechanical Coupled Loading. Journal of the American Ceramic Society, 2006, 89, 652-661.	3.8	62
101	Micromagnetic modeling studies on the effects of stress on magnetization reversal and dynamic hysteresis. Journal of Magnetism and Magnetic Materials, 2006, 301, 458-468.	2.3	30
102	Micromagnetic simulation of size effects on the properties of ferromagnetic materials. Journal Physics D: Applied Physics, 2006, 39, 1987-1992.	2.8	6
103	Three-dimensional phase field simulation for surface roughening of heteroepitaxial films with elastic anisotropy. Journal of Crystal Growth, 2005, 284, 281-292.	1.5	31
104	Strain-driven instability of a single island and a hexagonal island array on solid substrates. Surface Science, 2004, 553, 189-197.	1.9	10
105	Strain-mediated patterning of surface nanostructure by the subsurface island array. Journal of Crystal Growth, 2004, 269, 262-269.	1.5	4
106	Three-dimensional phase field modeling of phase separation in strained alloys. Materials Chemistry and Physics, 2003, 78, 442-447.	4.0	11
107	Ramified growth of two-dimensional islands due to misfit strain. Acta Materialia, 2003, 51, 4161-4170.	7.9	4
108	Spontaneous ordering of composition pattern in an epitaxial monolayer by subsurfacial dislocation array. Thin Solid Films, 2003, 440, 285-292.	1.8	9